New physics research at LHAASO

Xiao-Jun Bi (毕效军)
Institute of High Energy Physics, CAS

International Workshop on New Opportunities for Particle Physics 2024
IHEP, July 19 - July 22, 2024

LHAASO: Large High Altitude Air Shower Observatory

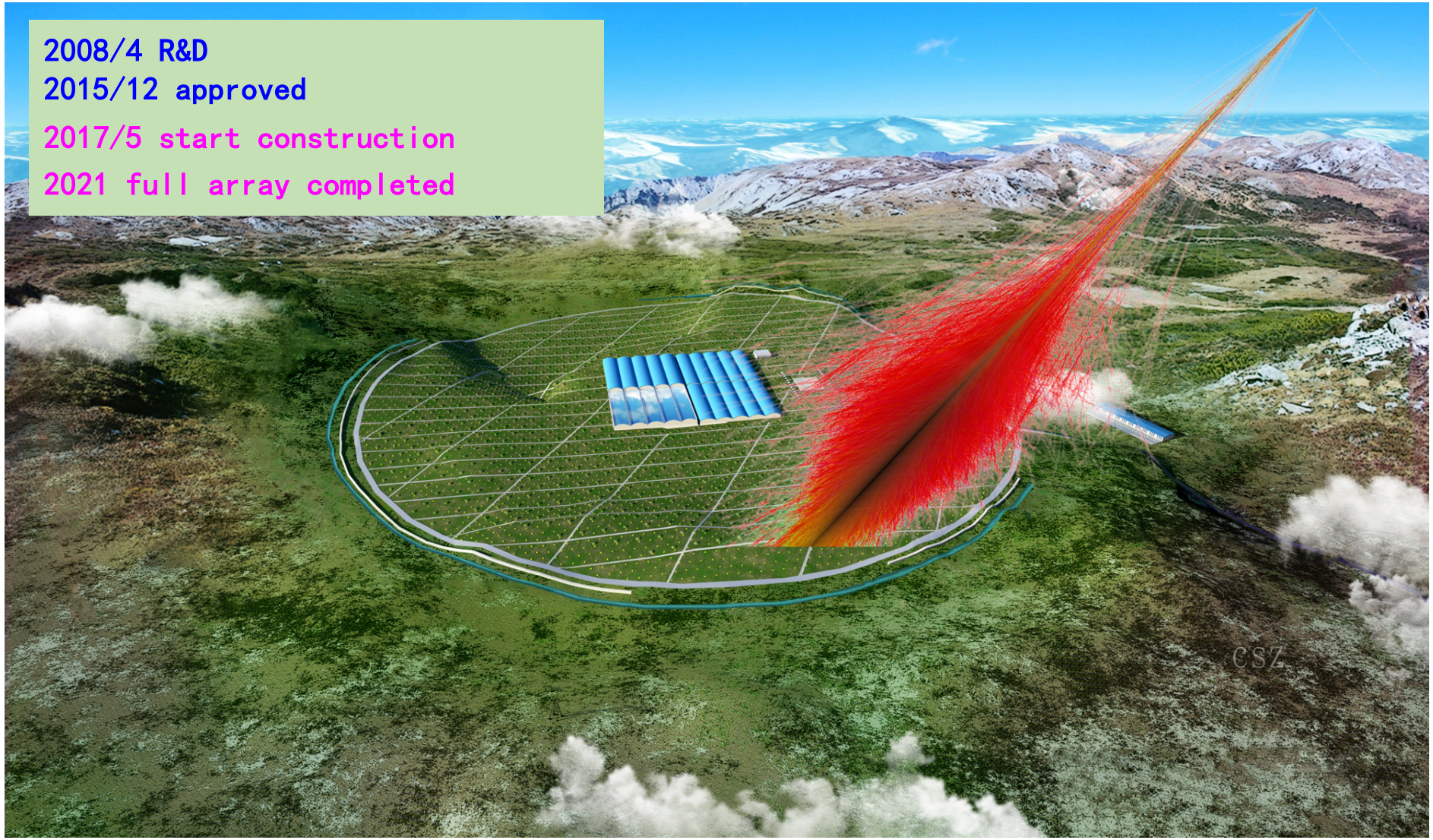

LHAASO aerial image, 2021/12

Haizi Mountain, Sichuan province, China

Altitude 4410 m a.s.l.

Area: 1.3km^2

LHAASO detectors

KM2A

MD: 1188x36m^2

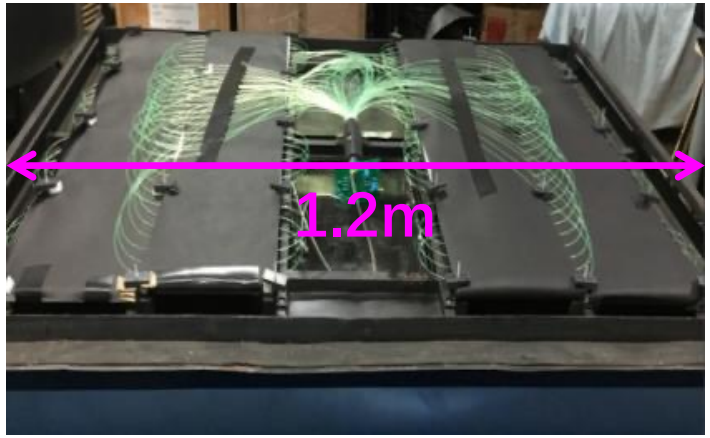

ED: 5216x1m^2

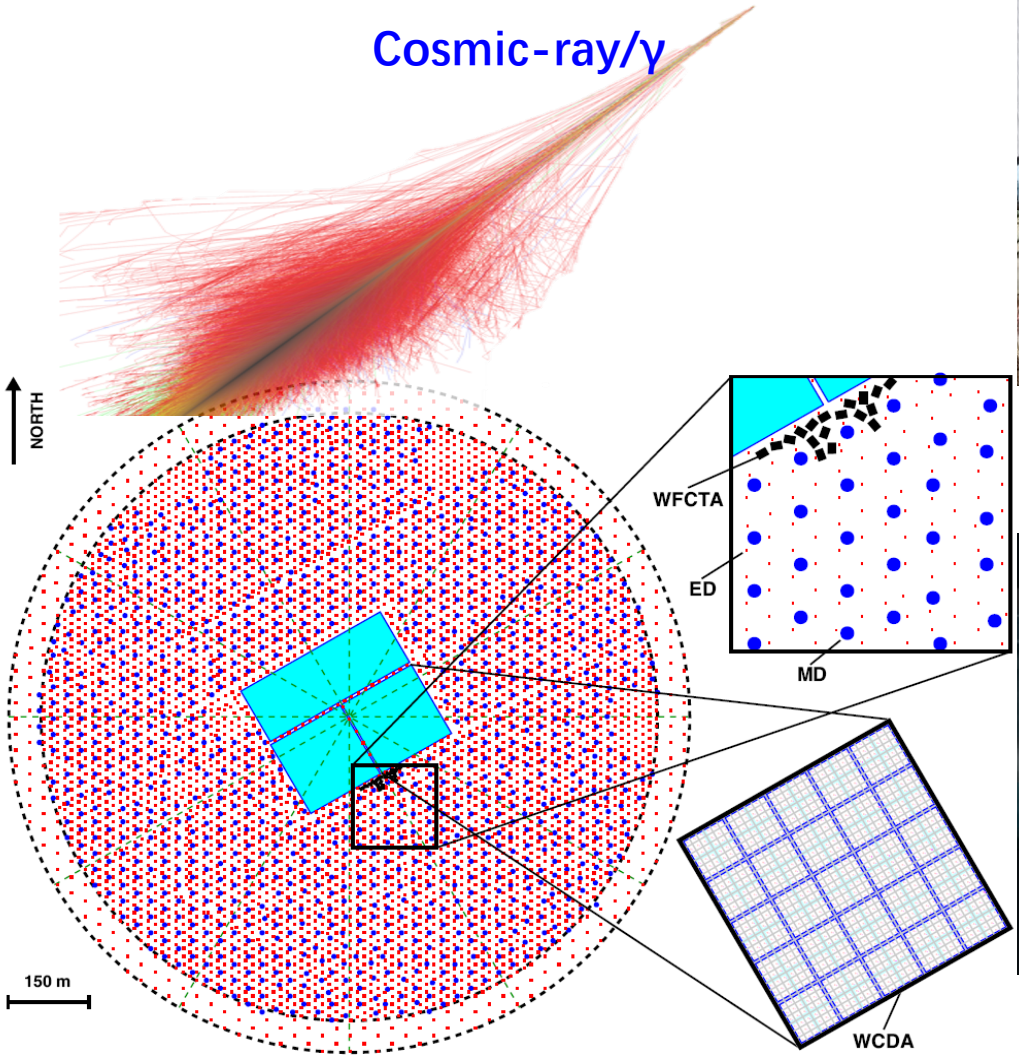

1.3 km^2

WFCTA

18x4.7m^2

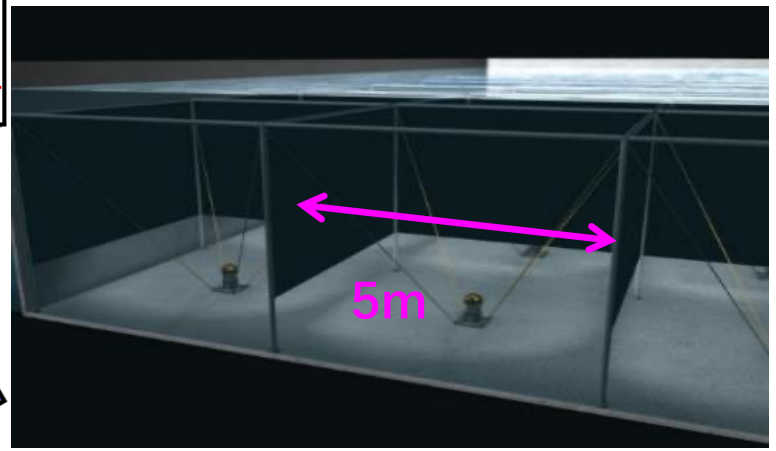

WCDA

3120x25m^2

Gamma-ray/cosmic ray discrimination

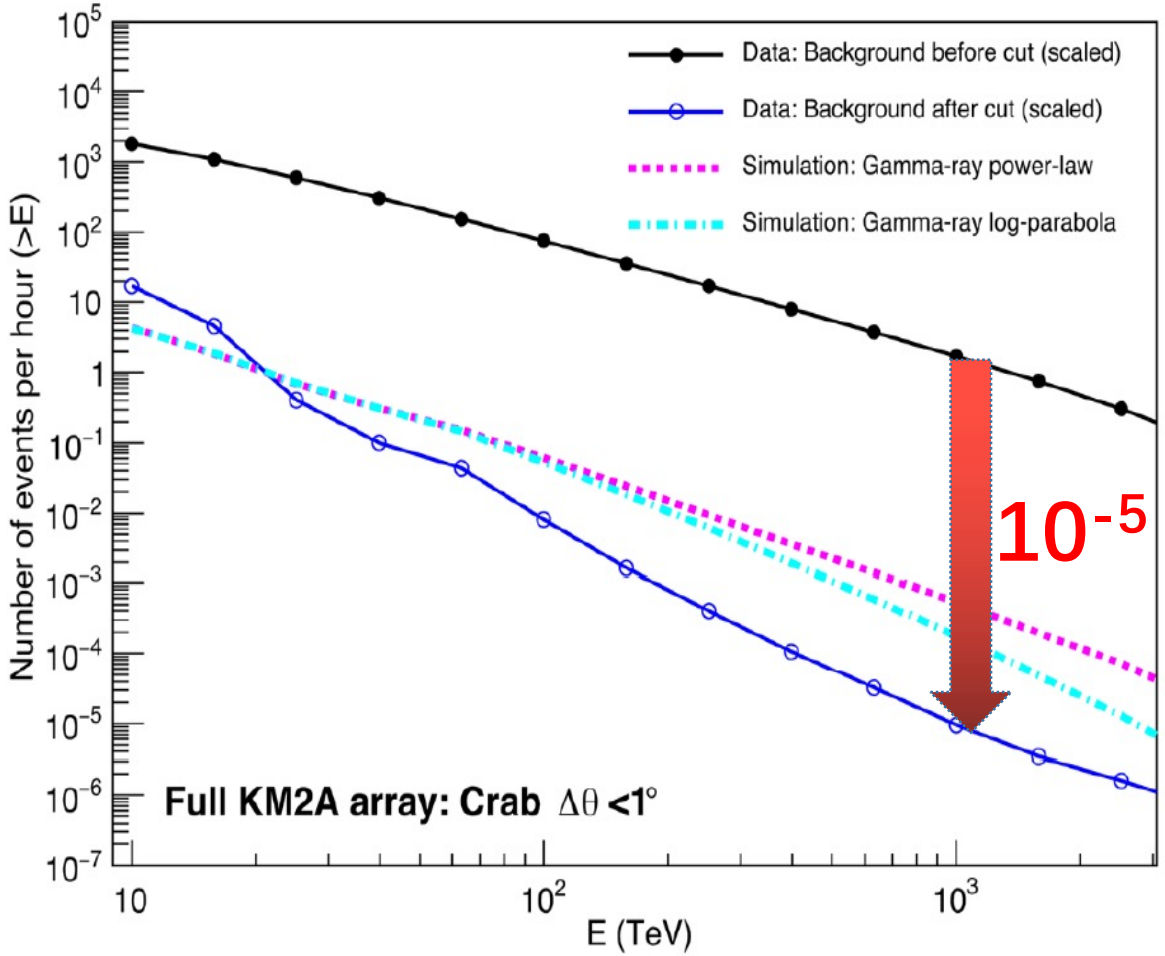

Before cut: CR rate

Gamma-ray rate

After cut: CR rate

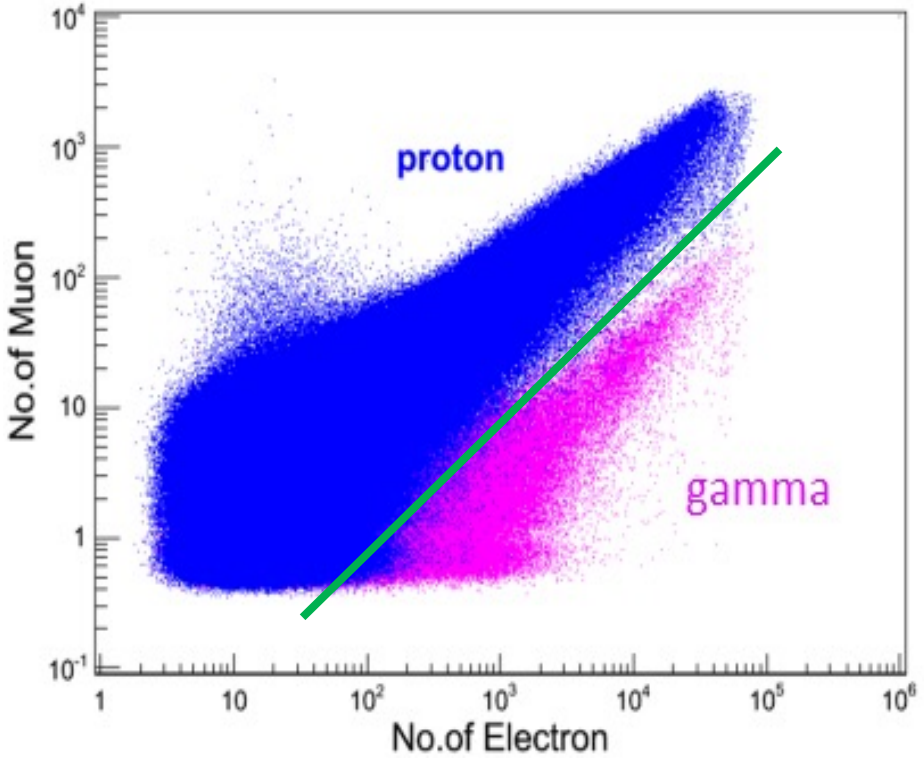

LHAASO for gamma-ray astronomy

- **Features : Large FOV, Full duty cycle, Wide energy, High sensitivity**
- **Important for: sky survey, extended sources, transient sources**

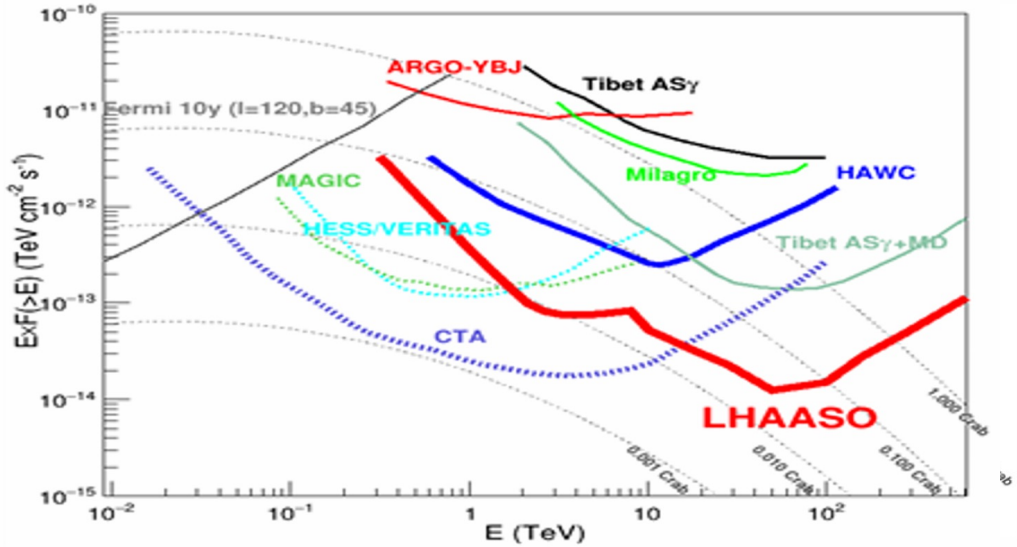

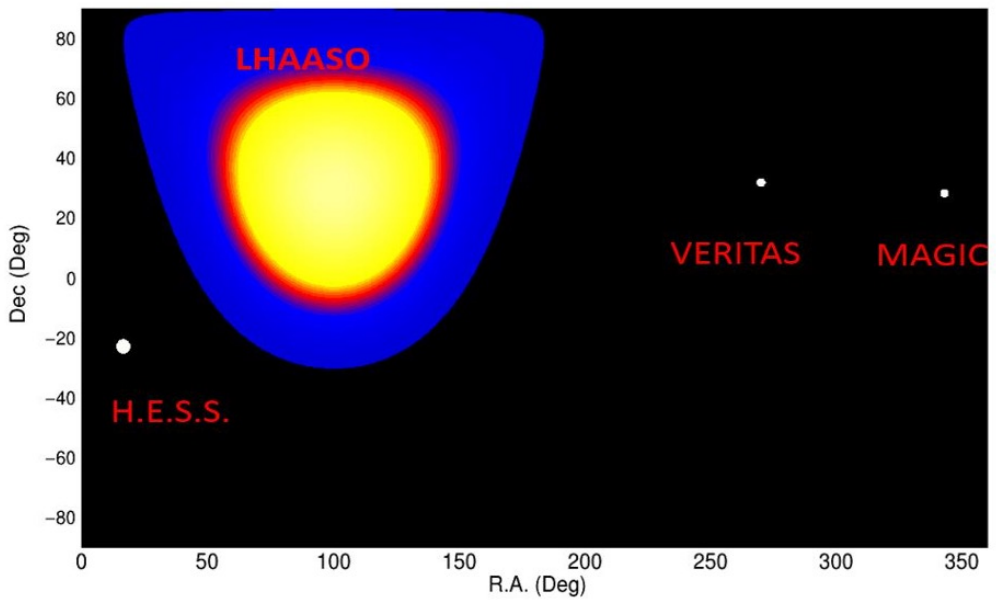

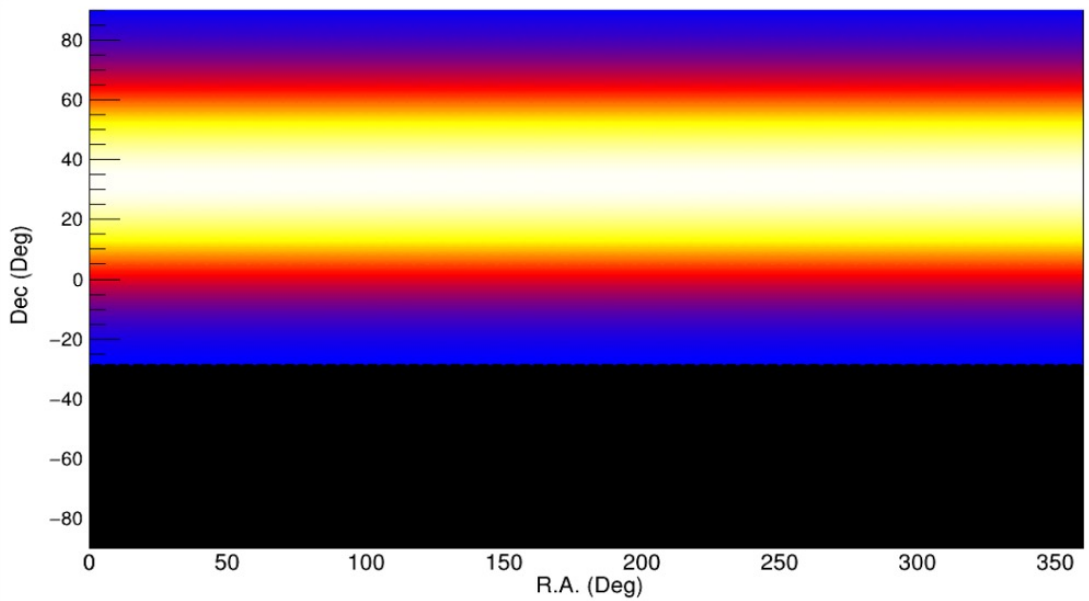

LHAASO important results

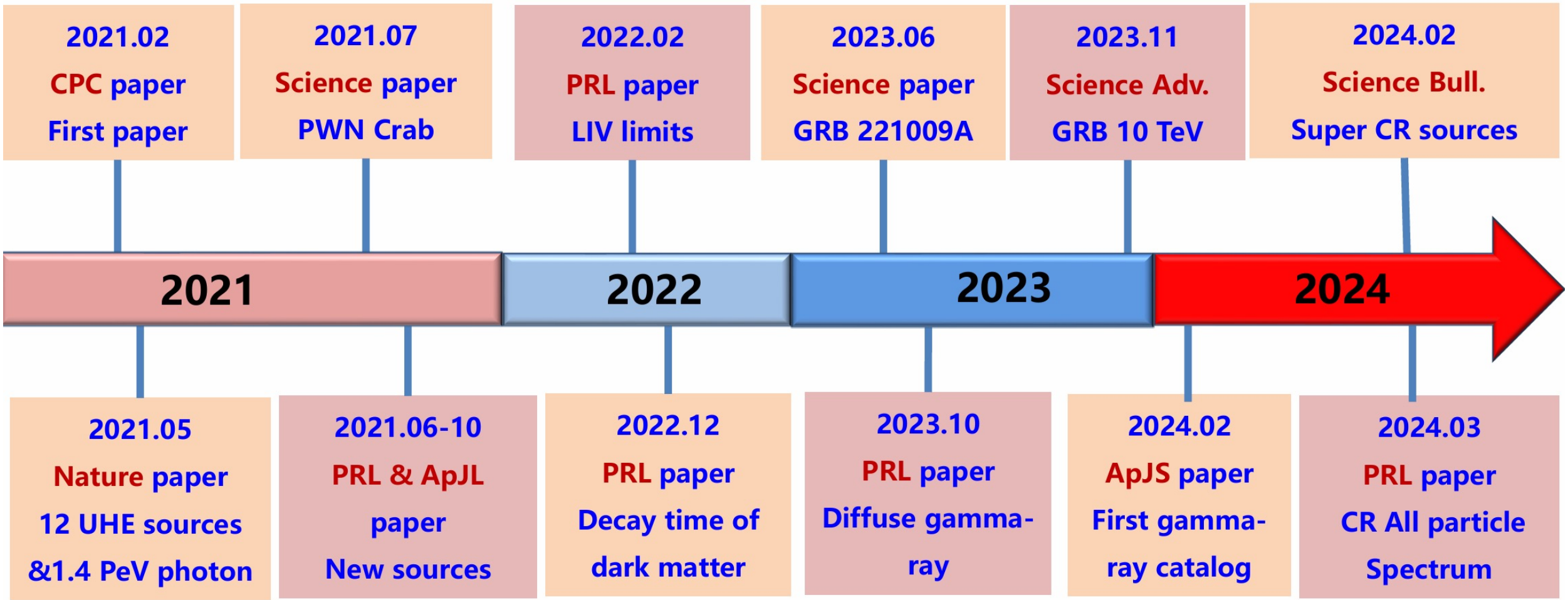

LHAASO probe of new physics beyond the standard model

- The SM is an extremely successful model that describes nearly all micro phenomena with a shocking accuracy. However it has many problems ……
- It doesn’ t account for the dark matter/dark energy ✓
- It can not explain why the world consists only normal matter but no antimatter.
- It has the strong CP problem.
  - Broken of PQ symmetry *predicts axion, which is a DM candida* ✓
- It has the hierarchical problem.
  - SUSY/extraD *generally predicts WIMP as dark matter.* ✓
- It does not include gravity.
  - Quantum gravity theories *which may indicate Lorentz invariance violation.* ✓
- ……

Dark matter searches

Superheavy DM decay from the Galactic halo

- The signal region is chosen ROI_0, around $15° \leq b \leq 45°$ and $30° \leq \ell \leq 60°$
  - Away from Galactic plane and Fermi bubble
  - Close to the GC as possible
- 4 control regions $\mathrm{ROI}_1 - \mathrm{ROI}_4$ by shifting ROI_0 along the RA direction by 90°, 135°, 240°, 285° respectively
  - Same declination and same detector performance
  - For accurate estimate the bkg and eliminate systematics

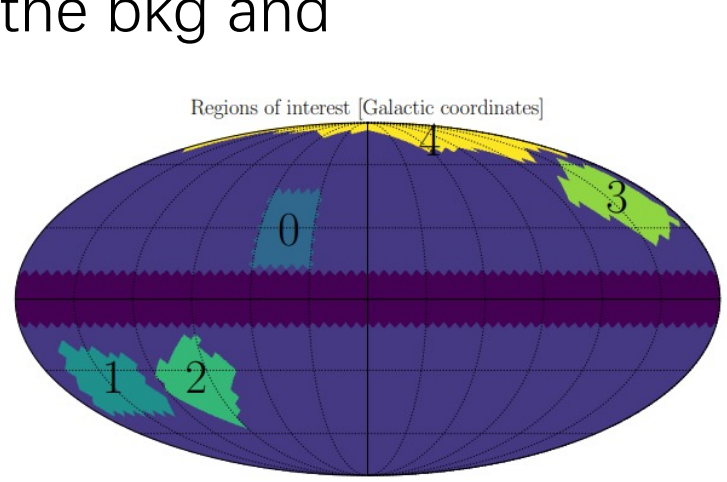

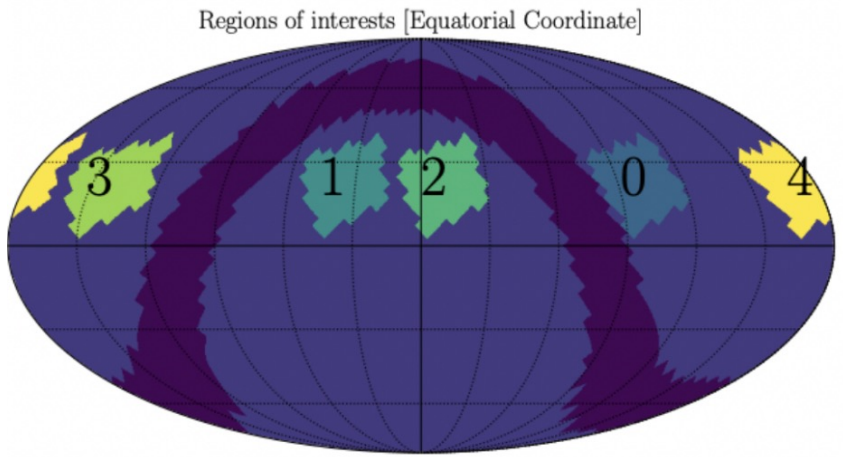

Likelihood analysis

- For each ROI
- $\ln L_k(\tau_{DM}, b) = \sum_i N_k^i \ln n_k^i - n_k^i$
- Combined likelihood
- $\ln L = \sum_{k=0}^{4} \ln L_k$

- Important features of this analysis

$$n_k^i(\tau_{\mathrm{DM}}, b) = (b^i + s_k^i(\tau_{\mathrm{DM}}))\mathcal{E}_k^i \Delta\Omega,$$

- The background model b^i, is independent of ROI
- Signal s_k^i , is different for each ROI, due to difference in D-factor
- We assume that we don't know b^i
  - allow it to be a free parameter (6 degrees of freedom)

Constraints on Heavy Decaying Dark Matter from 570 Days of LHAASO Observations

Phys.Rev.Lett. 129 (2022) 26, 261103

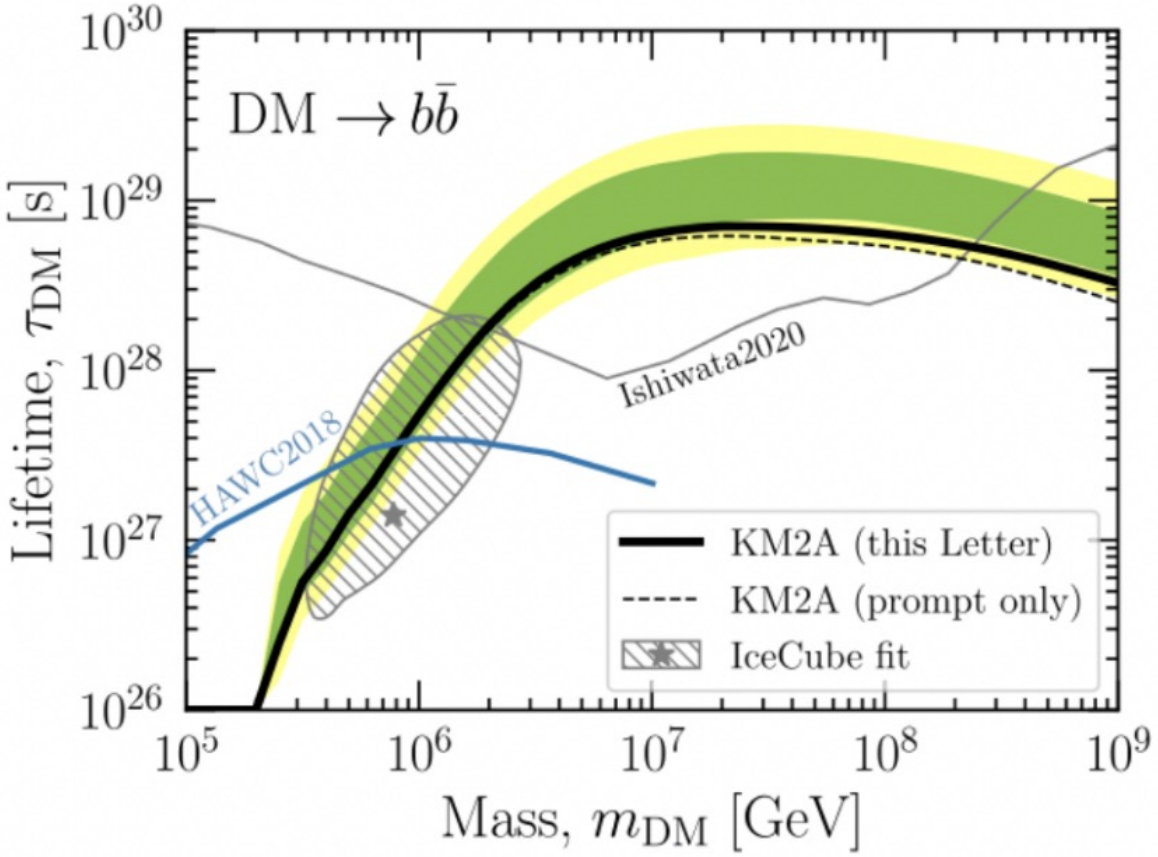

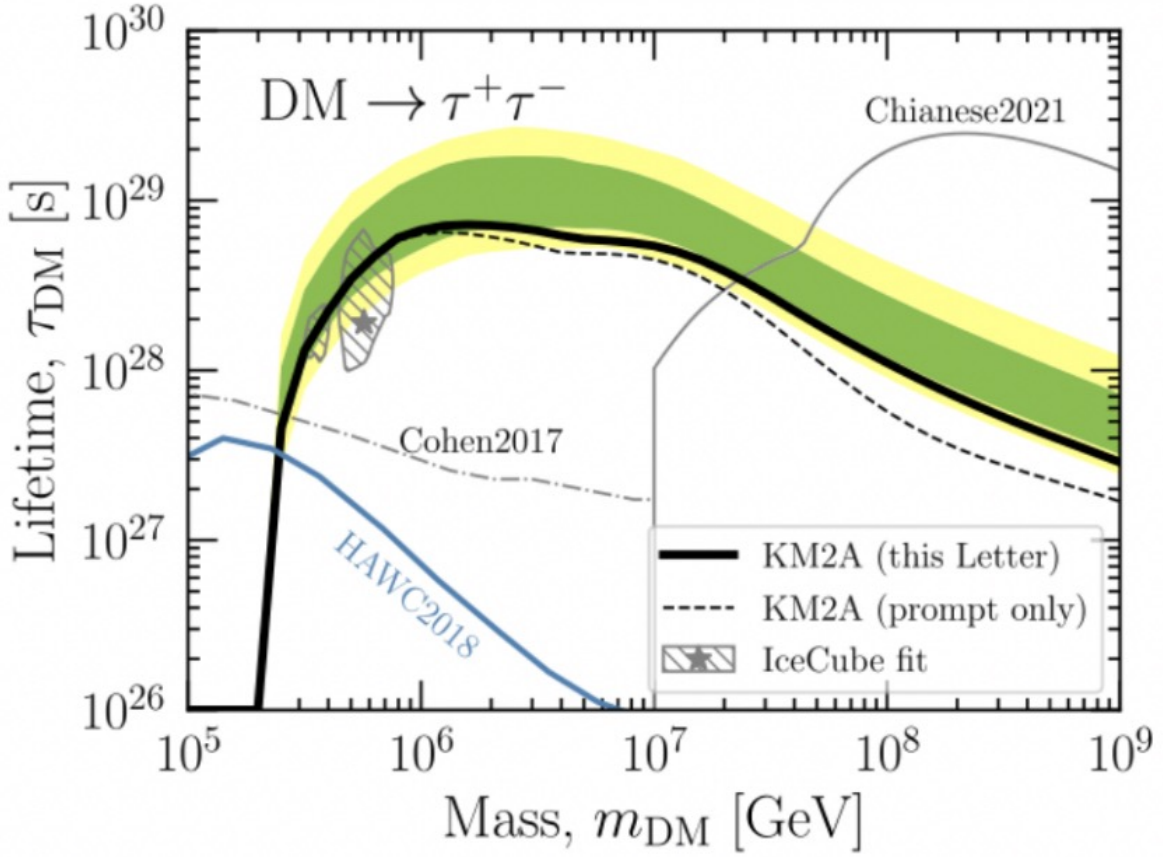

Dark matter annihilation signals from the dwarf galaxies

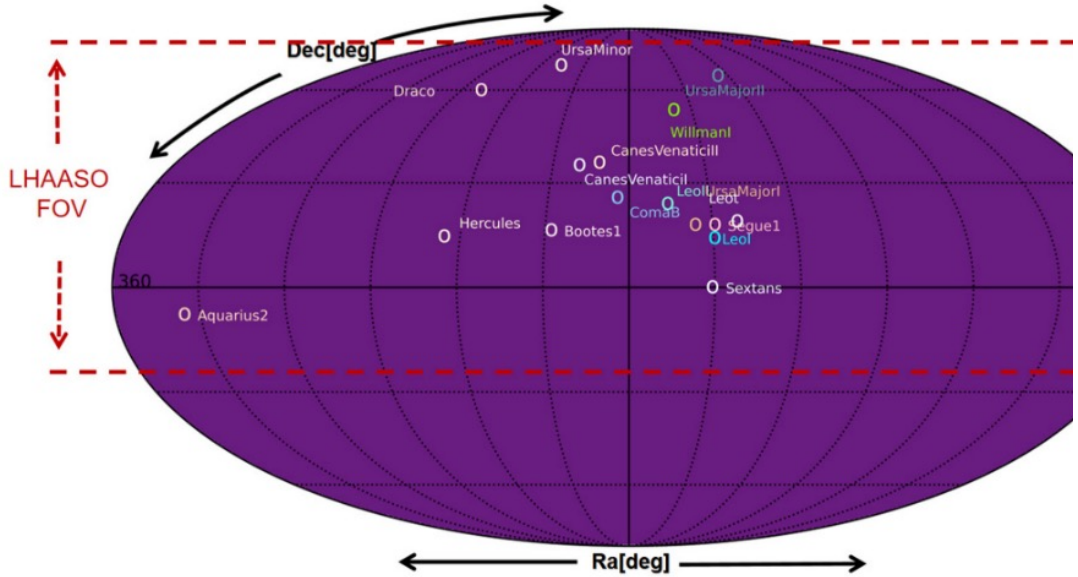

表 4.1　LHAASO（WCDA 和 KM2A）视场范围内 16 个矮椭球星系的赤经、赤纬和有效观测时间（天）

Name	RA[deg]	Dec[deg]	T_{WCDA}	T_{KM2A}
Draco	260.05	57.92	690.37	730.76
UrsaMinor	227.28	67.23	701.59	739.53
UrsaMajorI	158.71	51.92	692.51	742.17
UrsaMajorII	132.87	63.13	688.88	740.83
Bootes1	210.02	14.50	699.85	742.01
CanesVenaticiI	202.02	33.56	699.01	743.28
ComaB	186.74	23.90	696.88	744.34
LeoI	152.12	12.30	692.19	743.02
Segue1	151.77	16.08	691.72	743.06
Sextans	153.26	-1.61	693.36	743.60
CanesVenaticiII	194.29	34.32	698.15	743.81
Hercules	247.76	12.79	699.04	737.33
LeoII	168.37	22.15	693.95	744.18
WillmanI	162.34	51.05	693.45	742.21
Aquarius2	338.48	-9.33	666.84	728.11
LeoT	143.72	17.05	690.84	742.51

Density profile of DM in the dwarf galaxies

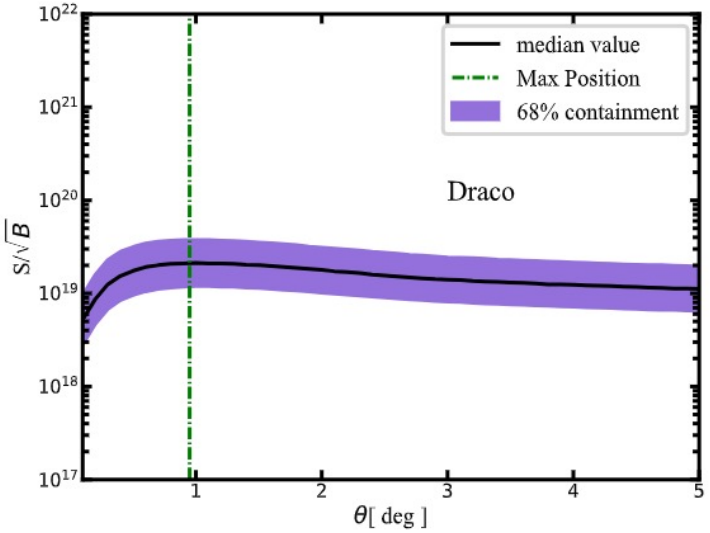

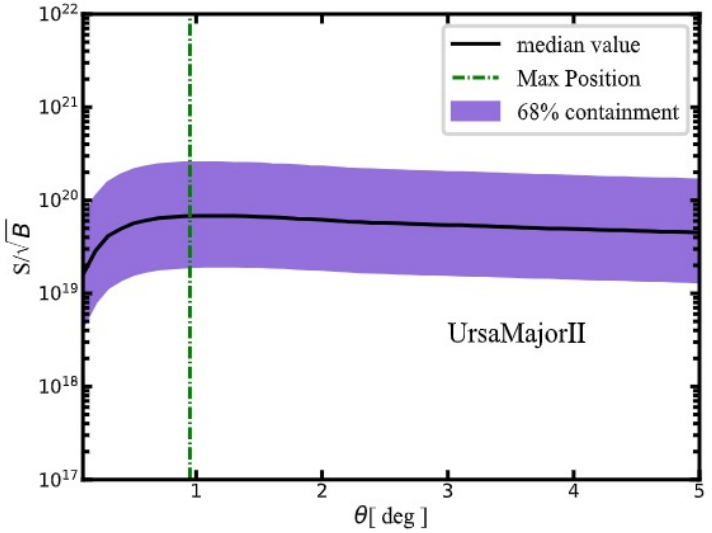

表 4.3　每个矮椭球星系的 J-因子的相应密度分布参数 [146]

Source	d/kpc	r_t/kpc	$\log_{10}(\rho_s/M_\odot \mathrm{kpc}^{-3})$	$\log_{10}(r_s/\mathrm{kpc})$
Draco	67.40	9.07	7.45	0.17
UrsaMinor	73.29	6.92	7.91	-0.18
UrsaMajorI	95.58	8.34	7.83	-0.19
UrsaMajorII	29.90	6.26	7.27	0.38
Bootes1	65.69	9.06	6.62	0.58
CanesVenaticiI	211.09	19.82	7.20	0.14
ComaB	42.31	5.14	7.57	0.06
LeoI	266.15	23.25	7.72	-0.09
Segue1	23.88	3.41	6.96	0.39
Sextans	89.63	11.88	6.32	0.65
CanesVenaticiII	166.26	29.91	6.50	0.70
Hercules	138.16	22.21	6.17	0.82
LeoII	242.44	19.15	7.95	-0.23
WillmanI	44.46	8.07	7.81	0.10
Aquarius2	107.50	24.46	6.59	0.78
LeoT	380.69	25.00	6.69	0.74

表 4.4　本次工作中考虑的 16 个矮椭球星系的 ROI 半宽度和 J-（D-）因子

Name	$\log_{10}(\mathrm{J}/\mathrm{GeV}^2\mathrm{cm}^{-5})$	θ_{anni}[deg]	$\log_{10}(\mathrm{D}/\mathrm{GeVcm}^{-2})$	θ_{decay}[deg]
Draco	$18.96^{+0.16}_{-0.15}$	1.0	$18.49^{+0.33}_{-0.41}$	2.3
UrsaMinor	$18.79^{+0.12}_{-0.11}$	1.0	$18.68^{+0.33}_{-0.15}$	2.1
UrsaMajorI	$18.4^{+0.28}_{-0.27}$	0.9	$18.6^{+0.48}_{-0.46}$	1.6
UrsaMajorII	$19.73^{+0.43}_{-0.42}$	1.1	$19.46^{+0.45}_{-0.59}$	2.2
Bootes1	$18.39^{+0.36}_{-0.37}$	0.9	$18.81^{+0.41}_{-0.56}$	2.0
CanesVenaticiI	$17.43^{+0.16}_{-0.15}$	0.8	$18.19^{+0.4}_{-0.39}$	1.3
ComaB	$19.26^{+0.30}_{-0.43}$	0.9	$19.19^{+0.48}_{-0.77}$	2.1
LeoI	$17.58^{+0.10}_{-0.10}$	0.8	$18.47^{+0.34}_{-0.43}$	1.5
Segue1	$19.25^{+0.60}_{-0.69}$	0.8	$18.48^{+0.78}_{-0.70}$	1.2
Sextans	$17.80^{+0.10}_{-0.10}$	1.0	$18.49^{+0.28}_{-0.21}$	1.8
CanesVenaticiII	$17.87^{+0.38}_{-0.37}$	0.8	$18.48^{+0.51}_{-0.75}$	1.5
Hercules	$17.6^{+0.53}_{-0.69}$	0.8	$17.84^{+0.66}_{-0.64}$	1.2
LeoII	$17.72^{+0.18}_{-0.17}$	0.8	$17.85^{+0.62}_{-0.40}$	1.0
WillmanI	$19.8^{+0.50}_{-0.52}$	0.9	$19.03^{+0.72}_{-0.94}$	1.6
Aquarius2	$18.57^{+0.50}_{-0.57}$	1.1	$18.6^{+0.64}_{-0.71}$	1.6
LeoT	$17.66^{+0.55}_{-0.52}$	0.8	$17.9^{+0.66}_{-0.70}$	1.1

TS distribution from different dwarf galaxies

Compute the 3-dimensional likelihood function, and the TS values of different dwarf galaxies.

$$\mathcal{L}_k = \prod_{i,j} \mathrm{Poisson}(N^{obs}_{i,j,k}; N^{exp}_{i,j,k}) \times \mathcal{G}(B_k; B^{obs}_k, \sigma_k),$$

其中,

$$\mathcal{G}(B_k; B^{obs}_k, \sigma_k) = \frac{1}{\ln(10) B^{obs}_k \sqrt{2\pi}\sigma_k} \times e^{-[\log_{10}(B_k) - \log_{10}(B^{obs}_k)]^2 / 2\sigma_k^2}.$$

$$TS_k = -2\ln\left(\frac{\mathcal{L}_k(S=0)}{\mathcal{L}_k(S_{max})}\right),$$

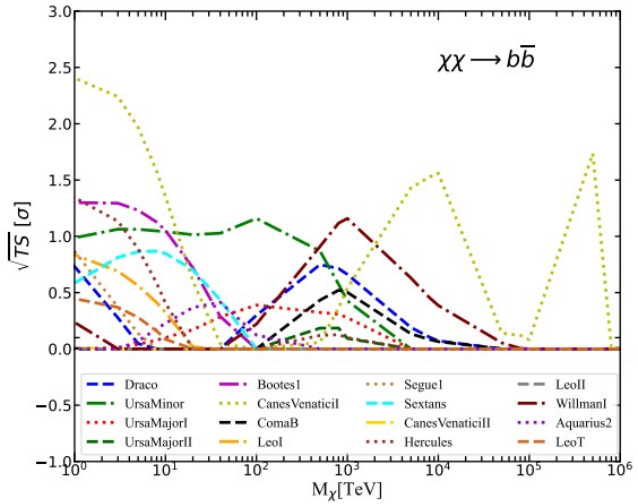

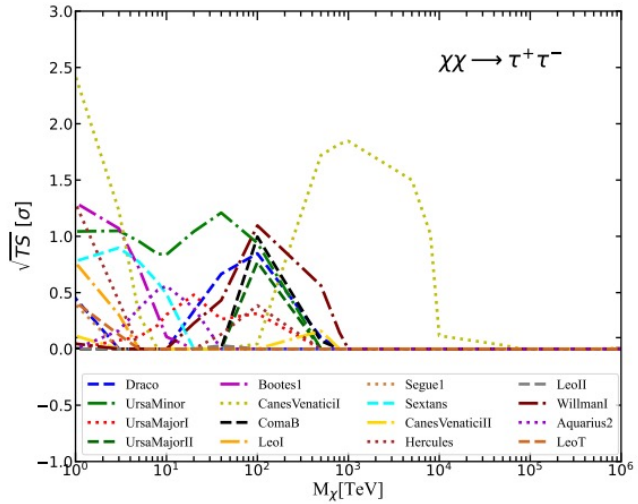

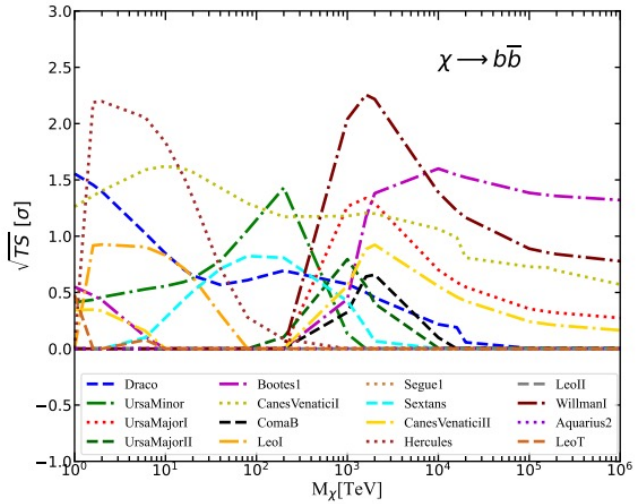

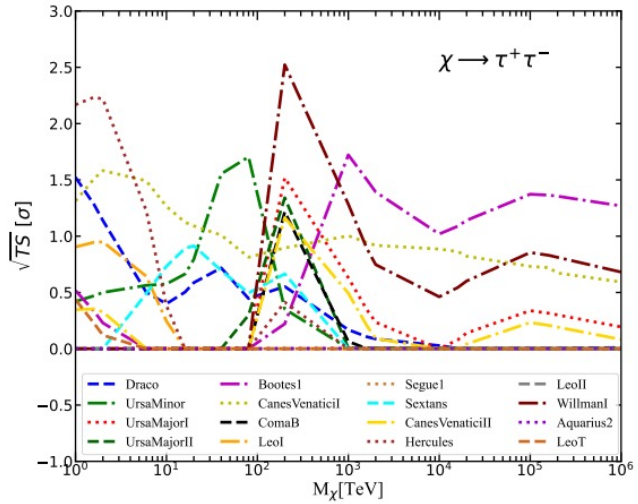

Most stringent constraint on heavy DM annihilation by LHAASO

Phys.Rev.Lett. 2024

- With 756 dates WCDA and 794 dates KM2A data and by combining the 16 dwarfs the most stringent constraint on DM annihilation is derived.

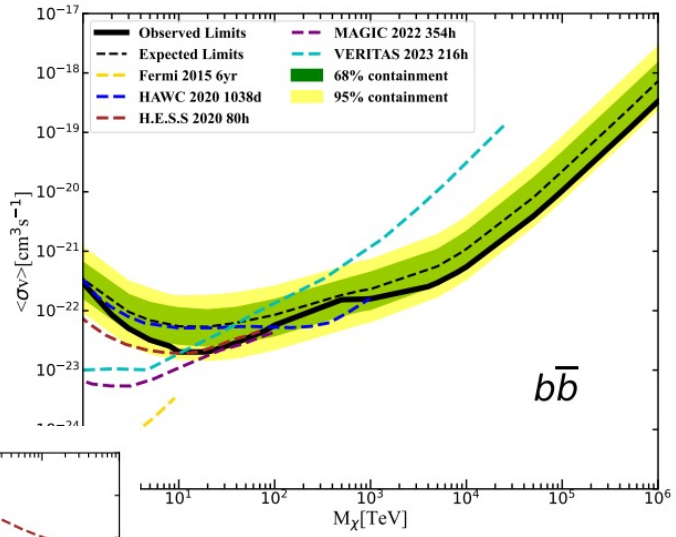

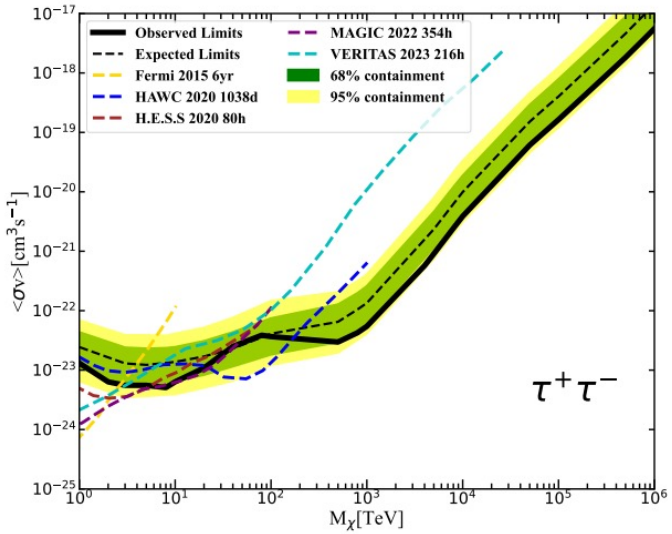

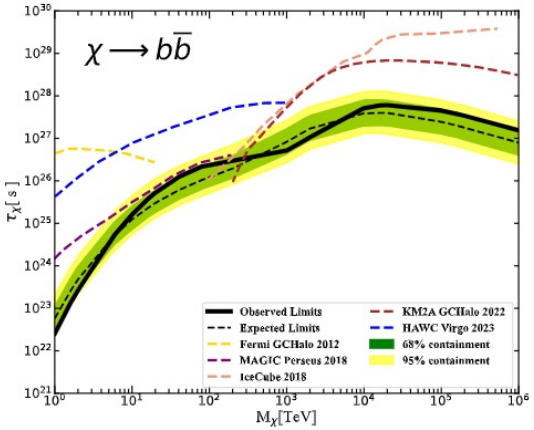

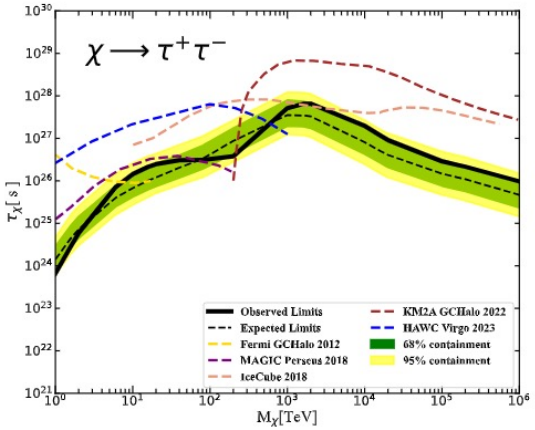

GRB 221009A and axion

LHAASO observation of GRB 221009A (BOAT)

LHAASO coll. Science,380:1390 (2023)

LHAASO coll. 2023 (Science adv. 9, 2778)

- Direct observation of the EBL absorption of gamma flux
- The highest energy photon is about ~13TeV, depending on the spectrum
- The 13 TeV event is out of expectation for source at z=0.151. Flux is about 1 order of magnitude higher than expectation.

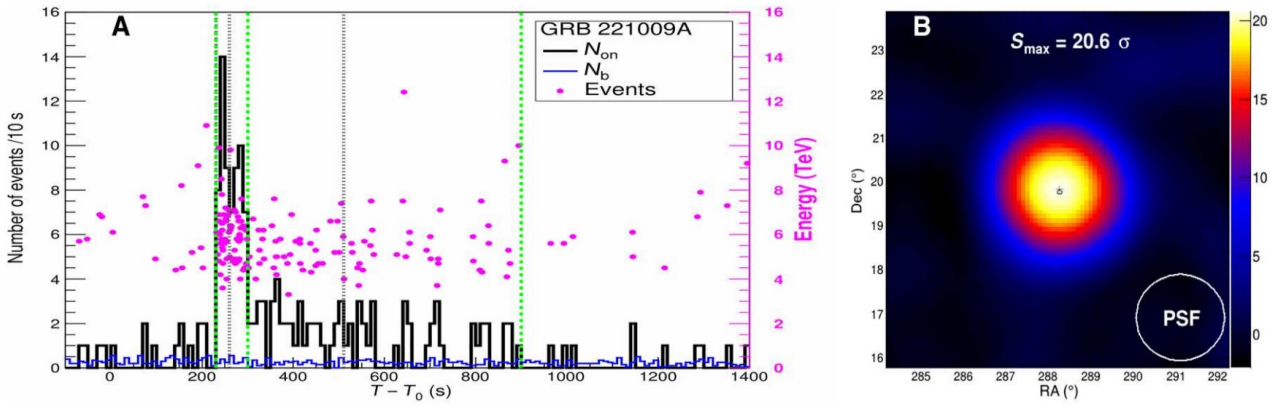

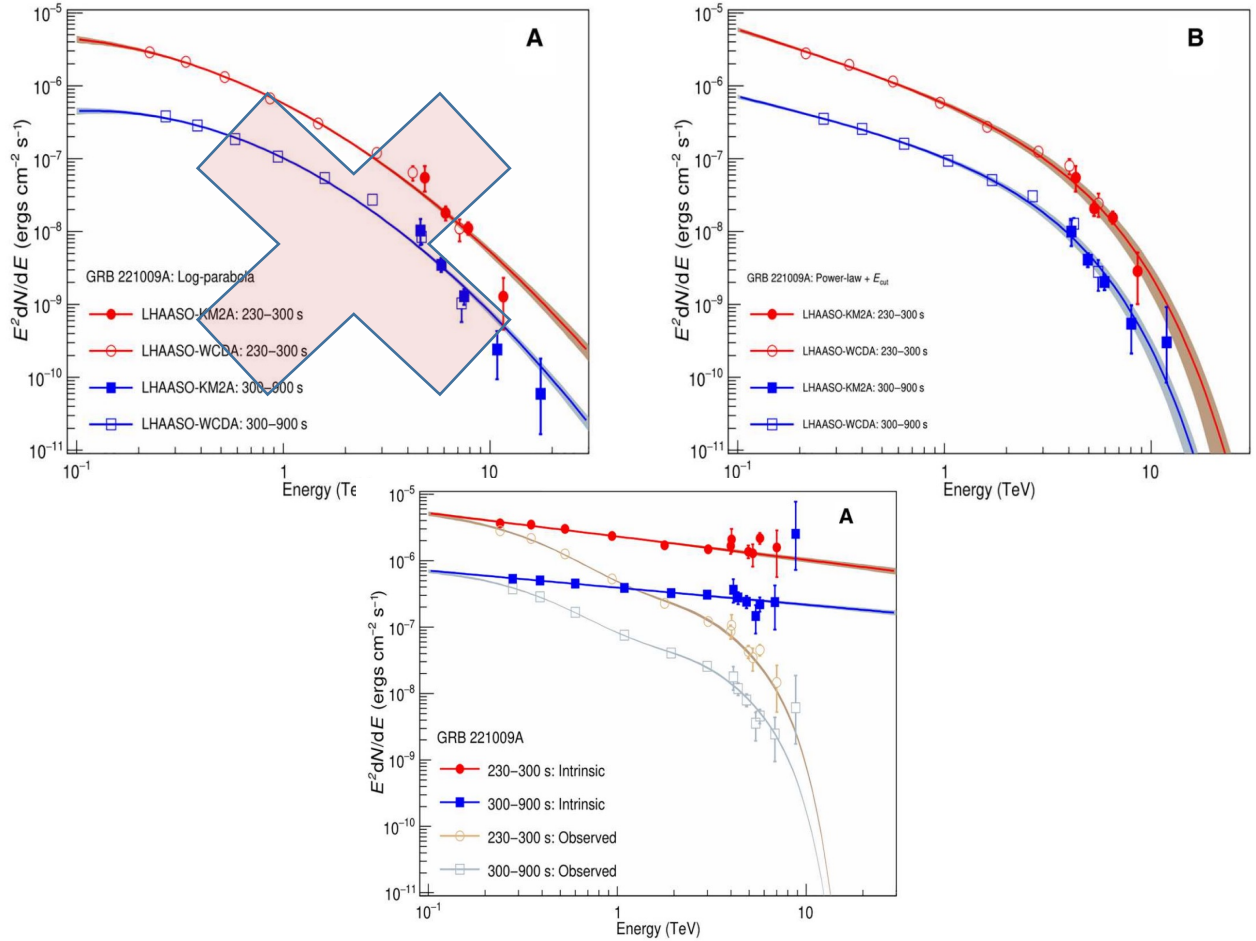

gamma-axion oscillation

- Oscillation between axion-gamma evade the absorption by EBL

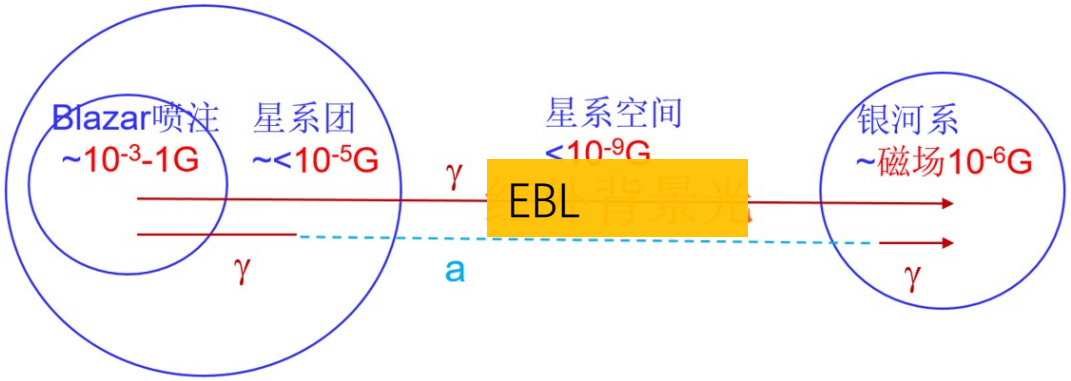

- The gamma ray spectrum is modified

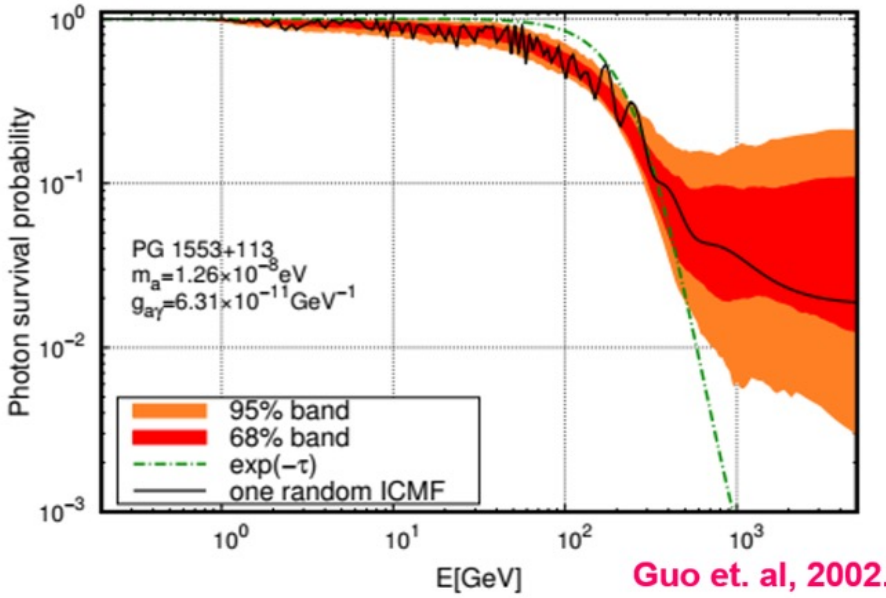

Guo et. al, 2002.07571

Best fit of axion scenario

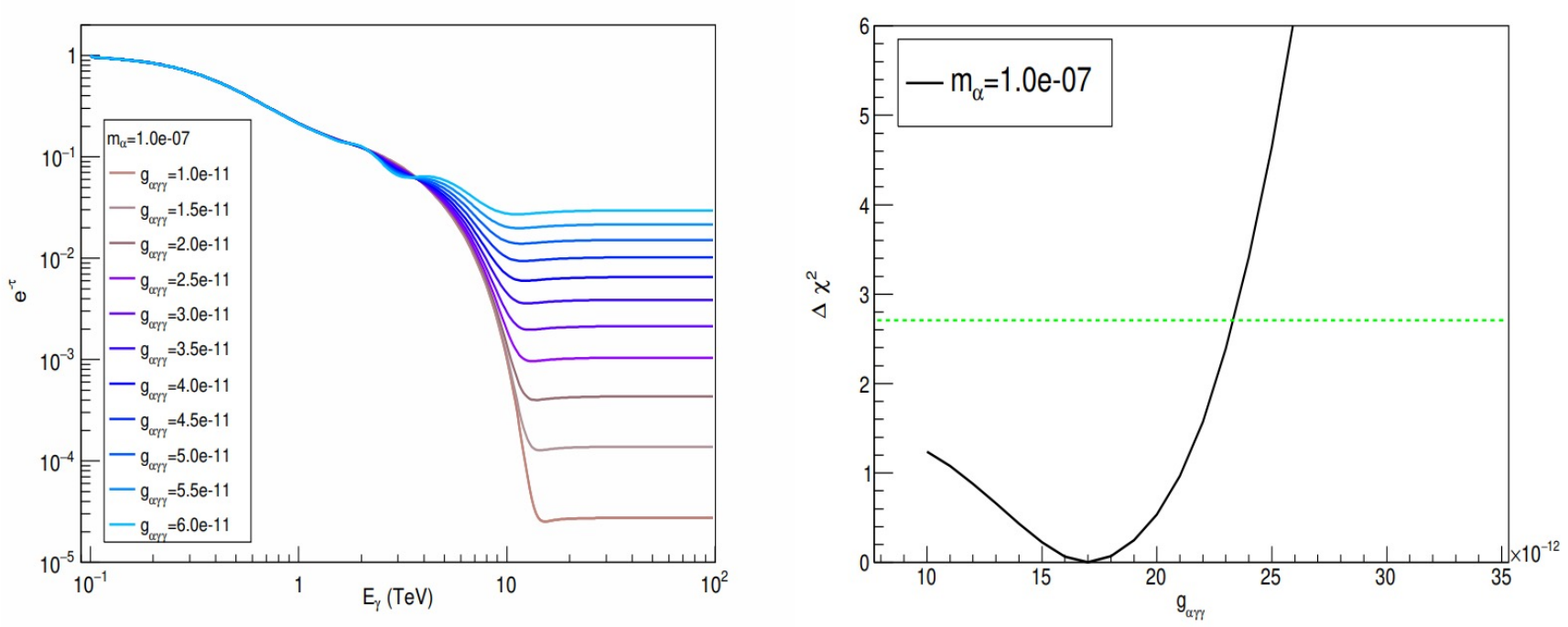

Figure S2: **The EBL absorption and the χ^2 of spectral fitting taking into account the ALP oscillation.** Panel A shows EBL absorption models for very high-energy gamma-rays from a redshift of $z = 0.151$, taking into account the oscillation between gamma-rays and ALPs assuming $m_a = 10^{-7}$ eV and $g_{a\gamma}$=(1 to 6)$\times 10^{-11}$ GeV^{-1}. The EBL model used is Saldana et al. 2021. Panel B shows $\Delta\chi^2$ relative to the minimum that fits the spectral energy distribution data as a function of the ALP $g_{a\gamma}$ for $m_a = 10^{-7}$ eV. The line indicates $\Delta\chi^2 = 2.71$ used to define the upper limit on $g_{a\gamma}$.

A stringent constraint is set on axion coupling

LHAASO coll. 2023 (Science adv. 9, 2778)

- Axion significance < 2sigma, we give constraints on axion coupling

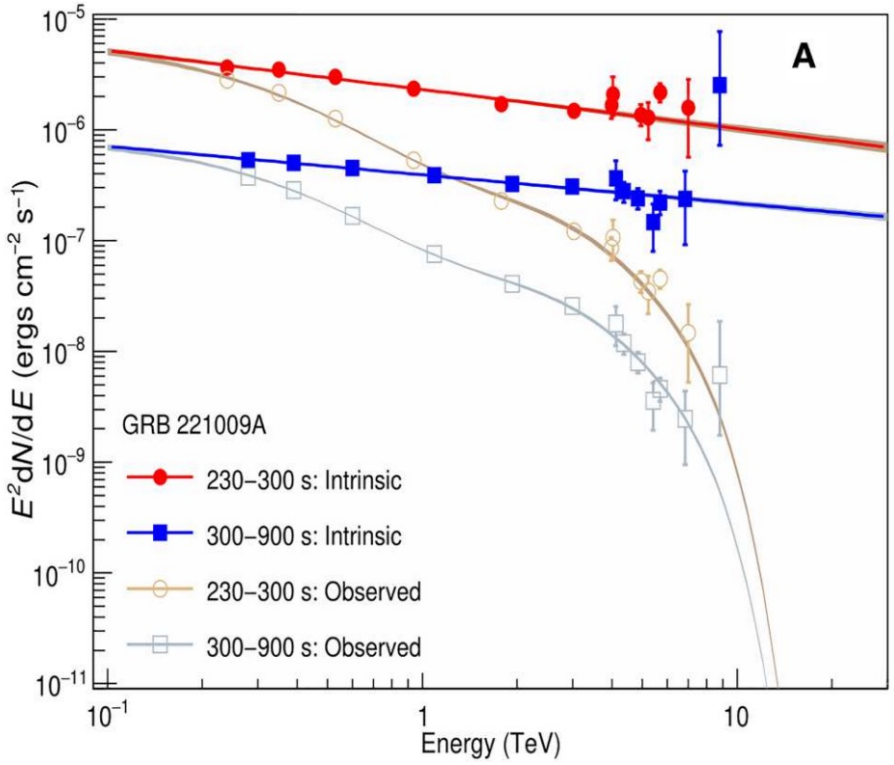

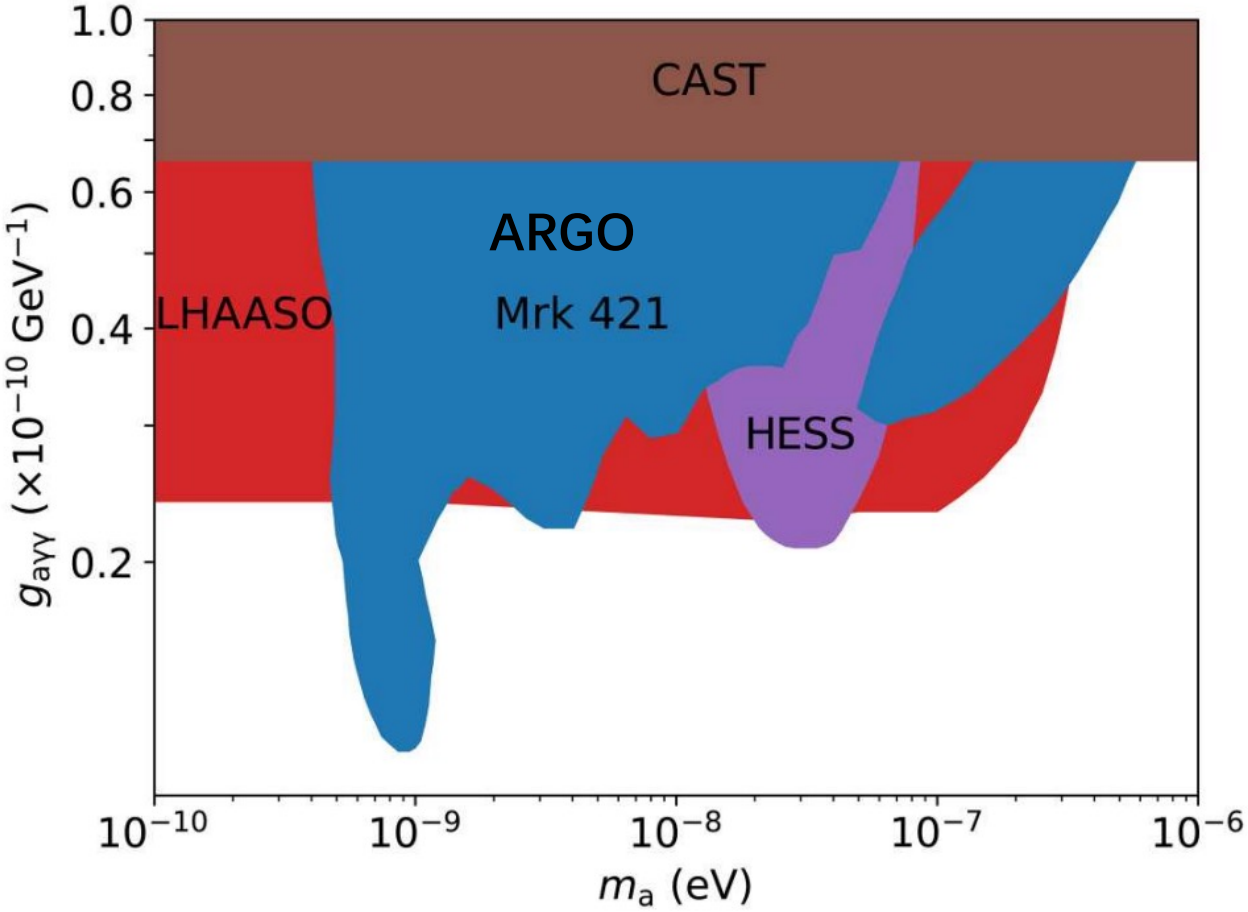

Constraints on Lorentz Invariance violation

Kinetics with LIV $E^2 = p^2 c^2 * (1 + a1(pc/ M_{pl} c^2) + a2(pc/ M_{pl} c^2)^2 + \cdots)$

- A free photon in vacuum is stable in LI; For LIV, if the effective mass of a photon $E_\gamma^2 - p_\gamma^2 = \frac{p^{n+2}}{E_{LIV}^n} = m_{\gamma,eff}^2$ is greater than a pair of e+e-, the photon decay γ -> e+e- very fast and leads to a sharp cutoff at the SED

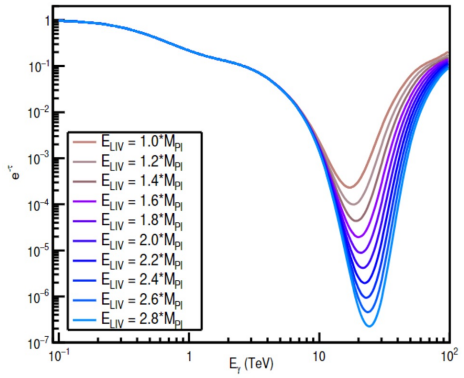

- Change the threshold of interaction. The threshold of γγ -> e+e- $\epsilon_{\rm thr} = \frac{m_e^2 c^4}{E} + \frac{1}{8}\left(\frac{E}{E_{\rm LIV}}\right) E$ is improved; more transparent of
- Energy dependent speed of light at LIV; v(E) = $\partial\omega / \partial k = \partial E / \partial p$ $\approx c\,(1 \pm \frac{1+n}{2}(E/E_{LIV,n})^n]$), it leads to time delay for different E from z,
- ⋯ others

$$\Delta t = \frac{\Delta z}{H_0} = \frac{1+n}{2H_0}\left(\frac{E_0}{\xi E_{pl}}\right)^n \int_0^z \frac{(1+z')^n dz'}{\sqrt{\Omega_m (1+z')^3 + \Omega_\Lambda}}$$

LHAASO发现的大于100 TeV的源

Z. Cao, et al., Nature 594, 33 (2021)

source name	R.A. (°)	dec (°)	Significance (σ) above 100 TeV	E_{Max} (PeV)	Flux ($\pm$ error) (CU) at 100 TeV
LHAASO J0534+2202	83.55	22.05	17.8	0.88 $\pm$0.11	1.00(0.14)
LHAASO J1825-1326	276.45	-13.45	16.4	0.42 $\pm$0.16	3.57(0.52)
LHAASO J1839-0545	279.95	-5.75	7.7	0.21 $\pm$0.05	0.70(0.18)
LHAASO J1843-0338	280.75	-3.65	8.5	$0.26\ ^{+0.16}_{-0.10}$	0.73(0.17)
LHAASO J1849-0003	282.35	-0.05	10.4	0.35 $\pm$0.07	0.74(0.15)
LHAASO J1908+0621	287.05	6.35	17.2	0.44 $\pm$0.05	1.36(0.18)
LHAASO J1929+1745	292.25	17.75	7.4	$0.71\ ^{+0.16}_{-0.07}$	0.38(0.09)
LHAASO J1956+2845	299.05	28.75	7.4	0.42 $\pm$0.03	0.41(0.09)
LHAASO J2018+3651	304.75	36.85	10.4	0.27 $\pm$0.02	0.50(0.10)
LHAASO J2032+4102	308.05	41.05	10.5	1.42 $\pm$0.13	0.54(0.10)
LHAASO J2108+5157	317.15	51.95	8.3	0.43 $\pm$0.05	0.38(0.09)
LHAASO J2226+6057	336.75	60.95	13.6	0.57 $\pm$0.19	1.05(0.16)

Photon decay or splitting

- LIV also leads to a photon decay or splitting to 3 photons

Decay : γ-> e+e-

$$E^{(1)}_{\rm LIV} \gtrsim 9.57 \times 10^{23}\ {\rm eV}\left(\frac{E_\gamma}{\rm TeV}\right)^3,$$

$$E^{(2)}_{\rm LIV} \gtrsim 9.78 \times 10^{17}\ {\rm eV}\left(\frac{E_\gamma}{\rm TeV}\right)^2.$$

Splitting: $\gamma \rightarrow 3\gamma$

$$\Gamma_{\gamma\to 3\gamma} = 5 \times 10^{-14}\frac{E_\gamma^{19}}{m_e^8 E_{LIV}^{(2)10}},$$

$$E^{(2)}_{LIV} > 3.33 \times 10^{19}{\rm eV}\left(\frac{L}{\rm kpc}\right)^{0.1}\left(\frac{E_\gamma}{\rm TeV}\right)^{1.9}.$$

- LIV decay or splitting leads to s sharp cutoff the high energy end of the spectrum
- We analyze the LHAASO data of gamma ray SED to look for the LIV cutoff

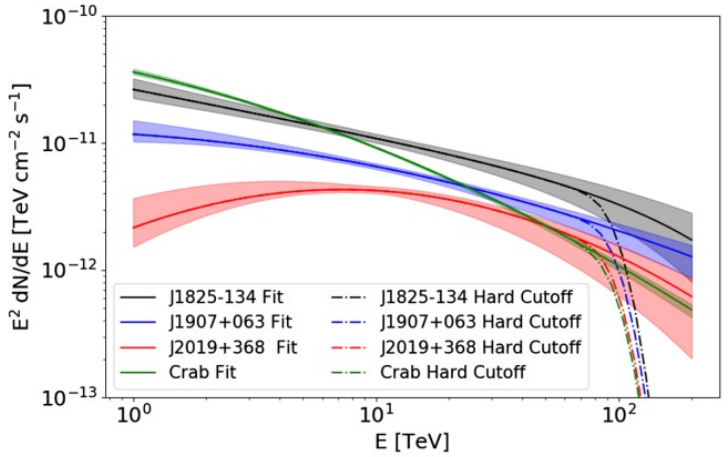

The result

Phys.Rev.Lett. 128 (2022) 5, 051102

Process: $\gamma \rightarrow e^+e^-$

$$E^{(1)}_{\rm LIV} \gtrsim 9.57 \times 10^{23}\ {\rm eV}\left(\frac{E_\gamma}{\rm TeV}\right)^3,$$

$$E^{(2)}_{\rm LIV} \gtrsim 9.78 \times 10^{17}\ {\rm eV}\left(\frac{E_\gamma}{\rm TeV}\right)^2.$$

Process: $\gamma \rightarrow 3\gamma$

$$\Gamma_{\gamma\to 3\gamma} = 5 \times 10^{-14}\frac{E_\gamma^{19}}{m_e^8 E^{(2)10}_{LIV}},$$

$$E^{(2)}_{LIV} > 3.33 \times 10^{19}{\rm eV}\left(\frac{L}{\rm kpc}\right)^{0.1}\left(\frac{E_\gamma}{\rm TeV}\right)^{1.9}.$$

Source	L (kpc)	$E_{\rm max}$ (PeV)	$E^{95\%}_{\rm cut}$ (PeV)	$E^{(1)}_{\rm LIV}$ (eV) $\times 10^{32}$	$E^{(2)}_{\rm LIV}$ (eV) $\times 10^{23}$	$E^{(2)}_{\rm LIV}$ (3γ) (eV) $\times 10^{25}$
Crab Nebula	2.0	0.88 ± 0.11	$0.75^{+0.04}_{-0.04}$	$4.04^{+0.69}_{-0.62}$	$5.5^{+0.61}_{-0.58}$	$1.04^{+0.11}_{-0.10}$
J2032+4102	1.4	1.42 ± 0.13	$1.14^{+0.06}_{-0.06}$	$14.2^{+2.42}_{-2.18}$	$12.7^{+1.41}_{-1.34}$	$2.21^{+0.23}_{-0.22}$

$E_{planck} = 1.22*10^{19}$ GeV

10^5 E_{planck}

0.1% E_{planck}

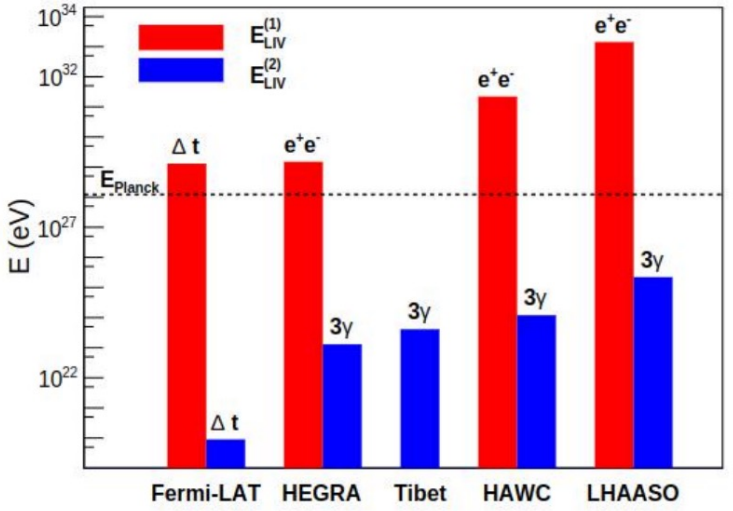

$E^{(1)}_{LIV}$和$E^{(2)}_{LIV}$限制提高了一个量级

LIV by GRB 221009A

- The intrinsic gamma spectrum shows a bump at the highest energy. It stimulates a lot of interests. LIV is a possible solution which leads to more transparent EBL.

- As the significance is not high. Constraint on LIV is set finally $E_{LIV} > 1.5\ M_{PI}$.

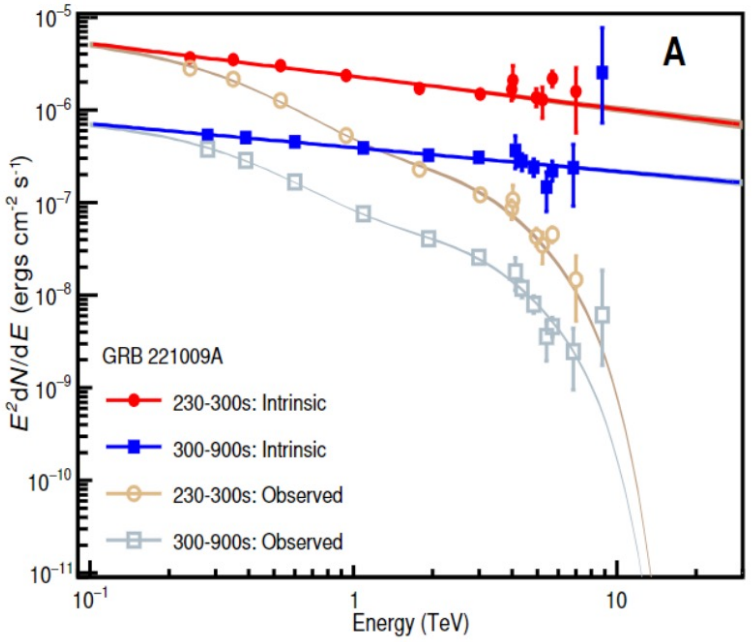

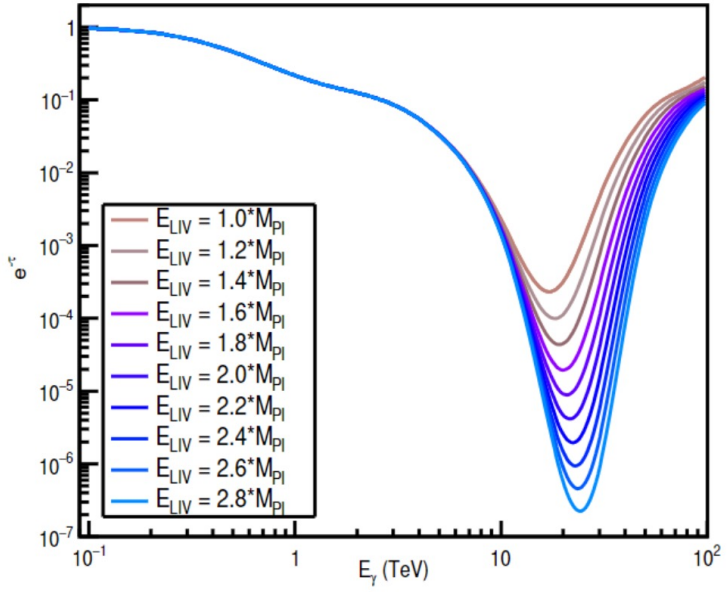

Constraint on LIV by time lag of different energy photons from GRB 221009A

- **Cross correlation function (CCF)**. Light curves of different energy bands are given by the WCDA data. CCF method is adopted to derive the time lags of the different light curves.
- **Maximal likelihood method**. The probability density function (PDF) of a photon at time t and N_{hit} is given. λ(t) is the intrinsic light curve with possible time lag $\Delta t_{LIV}(E)$.

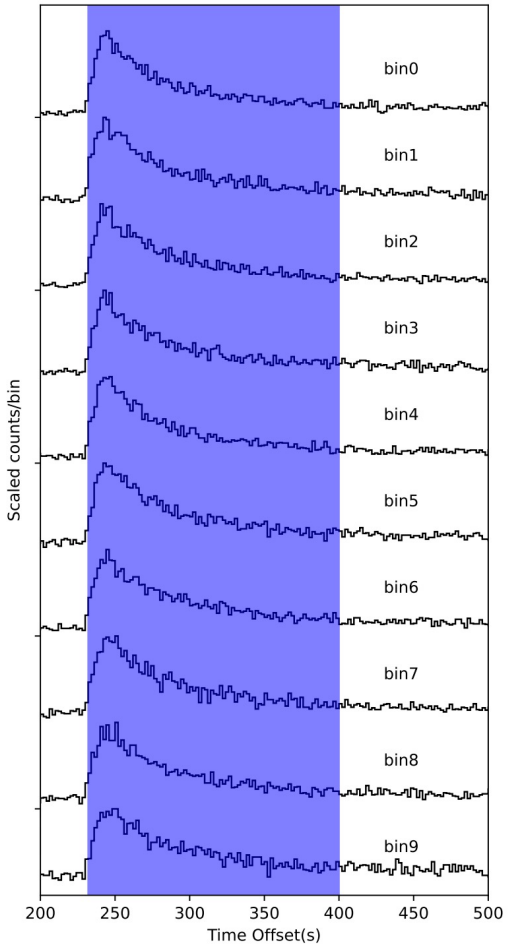

$$P\left(t, N_{\rm hit}|\eta_n,\ I\right) \propto \int_0^{\infty} \lambda\left[t - \Delta t_{\rm LIV}\left(E,\ \eta_n\right)\right]\gamma(E) \times F(E) A_{\rm N_{hit}}(E)\, dE;\ N_{hit} = 0, 1, ..., 9$$

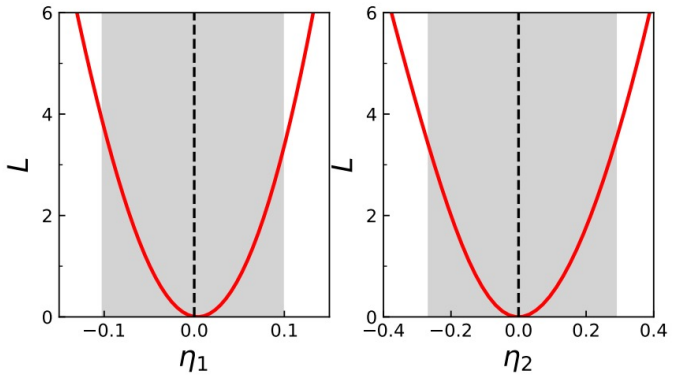

The stringent LIV constraint by time of flight

LHAASO Coll, PRL 2024

- For the 2nd LIV the LHAASO constraint is the best one with 6-8 times improvement to Fermi-LAT result.

Method	Cross correlation function			Maximum likelihood		
	η^{LL}	η^{BF}	η^{UL}	η^{LL}	η^{BF}	η^{UL}
η_1	−0.25	0.05	0.18	−0.10	0.00	0.10
η_2	−0.60	0.25	0.64	−0.27	0.00	0.29
	superluminal		subluminal	superluminal		subluminal
$E_{QG,1}[10^{20}\,GeV]$	0.5		0.7	1.2		1.2
$E_{QG,2}\,[10^{11}\,GeV]$	5.0		4.8	7.5		7.2

Summary

- LHAASO is a powerful instrument for gamma ray astronomy with large FOV, wide energy range, high sensitivity. It achieves impressive success.

- We have looked for dark matter signals, axion signals and LIV signals at LHAASO. No signals are observed and the strongest constraints are set on the new physics parameters.

- With the progress of the LHAASO observation and data accumulation we expect more important results will come. We hope LHAASO can provide a ‘new opportunity’ for new physics search complementary to colliders.

The photons with the maximum energy

- The energy of each photon depend on the true SED, which is SED model dependent.

$$P(E|(E_{rec},\theta)) = \frac{f(E)A_{eff}(E,\theta)P(E_{rec}|(E,\theta))}{\int f(E)A_{eff}(E,\theta)P(E_{rec}|(E,\theta))dE}$$

$$\xi = \int_0^{E_\xi} P(E|(E_{rec},\theta))dE$$

T_{event}(s)	E_{LP} (TeV)	E_{PLEC} (TeV)	E_{EBL} (TeV)	N_e	N_μ	θ (°)	$\Delta\psi$ (°)	D_{edge} (m)	P (%)
236.6	$12.7^{+6.2}_{-3.8}$	$9.7^{+3.3}_{-2.1}$	$9.8^{+3.1}_{-2.3}$	60.6	0	28.5	0.46	77	7.0
242.5	$10.5^{+5.0}_{-3.2}$	$8.3^{+3.0}_{-2.1}$	$8.4^{+3.2}_{-2.2}$	57.4	0	28.8	0.45	111	10
262.4	$12.6^{+5.5}_{-3.8}$	$9.5^{+3.4}_{-2.3}$	$9.6^{+3.3}_{-2.4}$	57.3	0	28.6	0.53	180	5.7
358.1	$10.0^{+4.8}_{-3.2}$	$7.4^{+3.1}_{-1.8}$	$7.9^{+3.3}_{-2.2}$	46.0	0	28.7	0.54	119	6.0
571.1	$9.4^{+5.1}_{-3.0}$	$7.4^{+2.6}_{-2.5}$	$7.7^{+3.0}_{-2.5}$	45.7	0	29.5	0.52	99	7.8
643.0	$17.8^{+7.4}_{-5.1}$	$12.2^{+3.5}_{-2.4}$	$12.5^{+3.2}_{-2.4}$	81.8	0.3	29.7	0.62	181	4.5
812.4	$11.1^{+5.9}_{-4.3}$	$7.4^{+3.6}_{-2.8}$	$7.6^{+3.9}_{-3.0}$	68.0	0	30.3	0.66	112	11
863.8	$12.9^{+6.1}_{-3.9}$	$9.2^{+3.0}_{-2.8}$	$9.7^{+3.2}_{-3.1}$	100.2	0.8	30.1	1.07	81	17
894.1	$13.6^{+6.1}_{-4.2}$	$9.7^{+3.4}_{-2.5}$	$10.4^{+3.3}_{-3.0}$	60.5	0	31.8	0.83	214	16

TITLE: GCN CIRCULAR
NUMBER: 32677
SUBJECT: LHAASO observed GRB 221009A with more than 5000 VHE photons up to around 18 TeV
DATE: 22/10/11 09:21:54 GMT
FROM: Judith Racusin at GSFC <judith.racusin@nasa.gov>